

# Structural modeling of dual-affinity purified Pho84 phosphate transporter

Jens O. Lagerstedt<sup>a,b</sup>, John C. Voss<sup>c</sup>, Åke Wieslander<sup>b</sup>, Bengt L. Persson<sup>a,b,\*</sup>

<sup>a</sup> Department of Chemistry and Biomedical Sciences, Kalmar University, S-391 82 Kalmar, Sweden

<sup>b</sup> Department of Biochemistry and Biophysics, Stockholm University, S-106 91 Stockholm, Sweden

<sup>c</sup> Department of Biological Chemistry, University of California School of Medicine, Davis, CA 95616, USA

Received 31 August 2004; revised 20 October 2004; accepted 4 November 2004

Available online 20 November 2004

Edited by Hans Eklund

**Abstract** The phosphate transporter Pho84 of *Saccharomyces cerevisiae* is predicted to contain 12 transmembrane (TM) regions, divided into two partially duplicated parts of 6 TM segments. The three-dimensional (3D) organization of the Pho84 protein has not yet been determined. However, the 3D crystal structure of the *Escherichia coli* MFS glycerol-3-phosphate/phosphate antiporter, GlpT, and lactose transporter, LacY, has recently been determined. On the basis of extensive prediction and fold recognition analyses (at the MetaServer), GlpT was proposed as the best structural template on which the arrangement of TM segments of the Pho84 transporter was fit, using the comparative structural modeling program MODELLER. To initiate an evaluation of the appropriateness of the Pho84 model, we have performed two direct tests by targeting spin labels to putative TM segments 8 and 12. Electron paramagnetic resonance spectroscopy was then applied on purified and spin labeled Pho84. The line shape from labels located at both positions is consistent with the structural environment predicted by the template-generated model, thus supporting the model.  
© 2004 Published by Elsevier B.V. on behalf of the Federation of European Biochemical Societies.

**Keywords:** Dual-affinity purification; FLAG epitope; Electron paramagnetic resonance; Phosphate transport; Pho84; Yeast

## 1. Introduction

In the yeast *Saccharomyces cerevisiae*, the Pho84 protein is the primary inorganic phosphate transporter at conditions when the external availability of this nutrient is limited (for a recent review, see [1]). At such conditions, the *PHO* regulon (reviewed in [1,2]) upregulates the expression of the *PHO84* gene [3] and the synthesized protein is routed to the plasma membrane [4] where it is active in proton coupled phosphate transport [5]. The Pho84, belonging to the family of phosphate:proton symporters (TC No. 2.A.1.9; [6]), is a member of the major facilitator superfamily (MFS; [7,8]). The Pho84 (587 amino acid residues) is predicted to consist of 12 transmembrane (TM) segments, which can be seen as two homolo-

gous sequence segments each containing 6 TM regions that are separated by a predicted large central loop. This organization, likely reflecting ancestral gene duplication, appears to be common among the MFS proteins [9–11]. Recently, the three-dimensional (3D) structure of two other MFS proteins, the lactose permease (LacY) and the glycerol-3-phosphate/phosphate antiporter (GlpT) of *Escherichia coli*, was determined to an atomic resolution of 3.5 Å [12] and 3.3 Å [13], respectively. These studies revealed that the postulated duplication seen in MFS proteins is indeed present in the 3D structure of the folded proteins.

In this communication, we focus on the structural aspects of the Pho84 protein. Our two-step affinity purification system of dual-tagged Pho84 expressed in *E. coli* is described together with the applied electron paramagnetic resonance (EPR) spectroscopy analysis. The first 3D structure model of the Pho84 protein, based on the published GlpT structure, is presented and discussed.

## 2. Materials and methods

### 2.1. Materials

Thio-specific nitroxide spin label (MTS-SL; (1-Oxyl-2,2,5,5-tetramethylpyrroline-3-methyl) methanethiosulfonate) was purchased from Reanal Finechemical (Budapest, Hungary). Horseradish peroxidase-conjugated anti-mouse-Ig-antibody (from sheep) and enhanced chemiluminescence detection kit were obtained from Amersham Bioscience, UK. Anti-Xpress antibody, plasmid pTrcHisB and *E. coli* TOP10F' cells were obtained from Invitrogen, The Netherlands. Anti-FLAG antibody, anti-FLAG resin and FLAG peptide were purchased from Sigma. Expand High Fidelity polymerase was from Roche. Oligonucleotide primers were purchased from TAG Copenhagen A/S, Denmark. Cybergene AB, Sweden, performed DNA sequence analyses.

### 2.2. Plasmid constructions

The *PHO84* gene was PCR amplified from genomic yeast DNA using sense (5'-GAGAGAGGATCCGATGAGTTCGTCATAAAGAT) and antisense (5'-GAGAGAGAATTCCTATTTATCGTCATCGTCTTTATAATCTGCTTCATGTTGAAGTTG) primers, which harbored the *Bam*HI and *Eco*RI endonuclease sequences, respectively. A stretch of DNA corresponding to the FLAG antibody epitope (DYKDDDDK) was also present, prior to the stop codon, in the antisense primer. PCR products were restriction digested with *Bam*HI and *Eco*RI and subsequently ligated in frame into a pTrcHisB plasmid that had been treated with the same enzymes. The resulting plasmid, pTrcHisB-His6/Xpress-PHO84-FLAG, was transformed into TOP10F' *E. coli* cells, plated on solid LB-ampicillin medium and incubated o/n at 37 °C. DNA sequence analysis was performed to verify the integrity of open reading frames of the positive colonies. The two single cysteine mutant constructs (S402C and L530C) were made in two consecutive PCRs, where the products of the first reactions were used as primers in the second amplification reactions. For this,

\*Corresponding author. Fax: +46 480 446262.

E-mail address: [bengt.persson@hik.se](mailto:bengt.persson@hik.se) (B.L. Persson).

**Abbreviations:** EPR, electron paramagnetic resonance; MFS, major facilitator superfamily; MTS, (1-oxyl-2,2,5,5-tetramethylpyrroline-3-methyl) methanethiosulfonate; SDSL, site-directed spin label; TM, transmembrane

oligonucleotide primers for the S402C (5'-TCTGCTGGTTGTTTACCTGGT) and for the L530C (5'-ATTTTCGCCTGTTTCATGTTG) mutations were used, together with the above-mentioned *Bam*HI and *Eco*RI primers. The previously described cysteine free *PHO84* [14] was used as template. The PCR products were ligated into plasmid pTrcHisB, transformed into TOP10F' cells and DNA sequence confirmed as described above.

### 2.3. Expression in *E. coli*

Cells harboring the different plasmid constructs were cultivated o/n in 150 ml LB medium supplemented with 50 µg/ml ampicillin. The full volume was transferred to a broad-based 2.8 liter Erlenmeyer flask and mixed with 1.5 liter Terrific Broth (50 µg/ml ampicillin) medium giving a spectral absorbance of about 0.1 at 600 nm ( $A_{600}$ ). The culture was grown aerobically at 200 rpm and 30 °C. At an  $A_{600}$  of 0.6, 1 mM isopropyl 1-thio-β-D-galactopyranoside (IPTG) was added. After 6 h of induction, cells were harvested by centrifugation at 8000 × *g* for 10 min. Cell pellets were stored at –80 °C.

### 2.4. Extraction of protein

Cells thawed on ice were resuspended in 40 ml sterile-filtered buffer A (50 mM Tris–HCl (pH 7.6), 0.2 M NaCl, 10 mM MgCl<sub>2</sub>, 30 mM imidazole, 10% glycerol, and 0.1% Triton X-100; 0.45 µm filtered) to which lysozyme and 1 mM phenylmethylsulfonyl fluoride (PMSF) were added. Alternatively, where indicated, 50 mM sodium-phosphate replaced the Tris in buffer A. The suspension was incubated for 40 min at 4 °C. 10 ml portions of the chilled viscous suspension were sonicated for 20 s with a micro-tip sonicator. Triton X-100 and dodecylmaltoside were added to a final concentration of 0.4% and 0.1%, respectively, and the suspension was incubated for an additional 30 min at 4 °C followed by a repetition of the sonication step. Cell debris and unbroken cells were separated from solubilized protein by high-speed centrifugation for 30 min at 100000 × *g*. The filtrate (0.22 µm) supernatant was immediately used for dual-affinity purification.

### 2.5. Affinity purification

The protein extract (40 ml) was applied at a flow rate of 1 ml/min onto a 1 ml Hi-Trap column (Amersham Bioscience), connected on-line to a FPLC system and pre-charged with Ni<sup>2+</sup> according to the manufacturer's protocol. Buffer A with an imidazole concentration of 50 mM was used to prevent binding of protein contaminants having a low affinity for the resin. The enriched Pho84 protein was eluted with 300 mM imidazole in buffer A. The eluate (4 ml) was directly incubated with 200 µM MTS spin label at 4 °C for 30 min to generate spin-labeled protein (detergent-solubilized) and then applied onto the 1 ml anti-FLAG resin (Sigma) column, activated according to the manufacturer's protocol. After a second passage of the protein mixture, contaminants were washed out with 40 ml buffer A modified to contain no glycerol, imidazole or MgCl<sub>2</sub>. This allowed excess label to be efficiently removed. Finally, a gentle elution of the Pho84 was performed using 400 µg FLAG peptide (Sigma) dissolved in 4 ml glycerol, imidazole and magnesium free buffer A. The 4 ml fraction was concentrated to ~1 ml using a 4 ml capacity Ultrafree Centrifugal Filter with a 50 kD cutoff BIOMAX membrane (Millipore, Bedford, MA, USA). The sample was further concentrated to ~200 µl using a 0.5 ml capacity microspin concentrator (BIOMAX membrane) with a 10 kD cutoff.

### 2.6. EPR spectroscopy

EPR measurements were carried out in a JEOL X-band spectrometer fitted with a loop-gap resonator [15,16]. An aliquot (5 µl) of purified, spin-labeled protein was placed in a sealed quartz capillary contained in the resonator. Spectra of samples at room temperature (20–22 °C) were from a single 60-s scan over a field of 100 G at a microwave power of 2 mW and a modulation amplitude optimized to the natural line width of the individual spectrum (0.5–1.5 G).

### 2.7. Protein analysis

Samples of purified protein were mixed with sample buffer prior to separation by SDS–polyacrylamide gel electrophoresis using a 10% Laemmli system [17]. Immunoblotting was carried out on poly(vinylidene difluoride) membranes (Immobilon-P, Millipore) according to the Western Blotting Protocol (Amersham Bioscience). Use of anti-Xpress

(Invitrogen, The Netherlands) and anti-FLAG (Sigma) monoclonal mouse antibodies, and horseradish peroxidase-conjugated anti-mouse-Ig-antibody (Amersham Bioscience) allowed for immunological detection of the Pho84 proteins. After a short incubation with chemiluminescent substrates, the blot was exposed to film for 1 min.

Protein was assayed by use of the commercially available Bio-Rad D<sub>c</sub> Protein Assay kit (Bio-Rad) and bovine serum albumin was used as a standard.

### 2.8. Structural modeling of Pho84

Potential secondary and 3D structure models of the Pho84 protein were analyzed from its primary sequence by use of several local structure and fold recognition methods at the MetaServer (bioinfo.pl/meta/) [18] (i.e., PDB-Blast, 3D-Jigsaw, EsysPred3D, GRDB, FFAS03, SamT99, Superfamily, INBGU, FUGUE2, 3D-PSSM, mGenTH-READER, psipred, and profsec). These were jointly evaluated by the Pcons and 3D-Jury methods (at the same server). The established structure of the protein with the highest scores (GlpT; PDB code 1PW4) was used as template in the structural modeling of the Pho84 protein using the comparative modeling program MODELLER [19], in which the calculated 3D model was obtained by optimally satisfying spatial restraints derived from the 3D-Jury sequence alignment. The alignment of the Pho84 amino acid sequence with the GlpT sequence is from the evaluation of all the individual methods (cf. above) by the 3D-Jury system, where some loop regions had no fit. Analysis of the Pho84 structural model was performed by use of the DeepView/Swiss-PdbViewer program ([www.expasy.org/spdbv](http://www.expasy.org/spdbv)) and also by use of *Insight II* software (version 2000.1) on the Octane workstation by Silicon Graphics. The figures shown were produced by use of the latter.

## 3. Results and discussion

### 3.1. Pho84 structure model

From the Pho84 primary structure, a number of prediction and fold recognition methods (cf. Section 2) at the MetaServer (bioinfo.pl/meta/) [18] proposed substantial structural similarities to several MFS protein structures. Highly significant scores were given from the joint comparison of the individual methods by the 3D-Jury and Pcons evaluation systems (bioinfo.pl/meta/) for similarity to the *E. coli* glycerol-3-phosphate/phosphate antiporter (GlpT; PDB code 1pw4) and lactose permease (LacY; PDB code 1pv6) structures, and two theoretical structure models in the PDB database (human glucose transporter GLUT1 (PDB 1ja5a) and the *Plasmodium* hexose transporter PfhT1 (PDB 1lvia)). Both of the former two MFS proteins contain 12 TM domains and with extended central loops connecting the two homologous parts, and have superimposable TM parts of their structures [20]. Interestingly, both structures exhibited a pseudo twofold symmetry also on the 3D level [12,13]. The GlpT structure was used as a template for comparative modeling of the Pho84; its Pcons2 score (4.43) was similarly high as for a previous successful and validated structure model of a membrane surface protein [21]. The alignment between the two sequences was determined by the joint outcome from the individual methods, as shown by the 3D-Jury system, and illustrated in Fig. 1. The resulting 3D structure model with 12 TM regions is shown in Fig. 2(a). Generally, prokaryotic MFS proteins are smaller, with shorter loops and terminal extensions than eukaryotic members of the superfamily (discussed in [8]). Similarly, the GlpT is smaller than the Pho84 (452 vs. 587 amino acids). Based on the primary structure alignment (Fig. 1), it is obvious that the majority of the additional amino acids in the Pho84 structure constitute the comparatively long N- and C-terminal extensions (amino acids 1–37 and 557–587, respectively). These

Pho84	MSSVNKDTIHVAERSLHKEHLTEGGNMAFHNHLNDFAHIEDPLERRRLALESIDDEGFGWQVVKTI
1pw4_A	.....SIFKPAPHKARLPAAEIDPTYRRLRWQIF
1pv6a	.....FGLFFFF
1ja5_A	.....MEPSSKKLTGRMLAV
1lvi_A	MTKSSKD.....ICSENEGKKN.....GKSGFFSTSFKYV
Pho84	SIAGVGFLTDSYDIFAINLGITMMSYVYWHGSMFGPSQTLLKVSTSVGTVIGQFGFTLADIVGRK
1pw4_A	LGIFFGYAAYYLVRKNFALAMPYLVEQ....GFSRDLGFGALSGISIAYGFSKFMGVSVDNRNPR
1pv6a	YFFIMGAYFPFFPIWLHDIN.....HISKSDTGIIFAAISLFSLLFQPLFGLLSDKIGLR
1ja5_A	GGAVLGSLQFGYNTGVIN...APQKVIEEFSILPTTLTTLTSLVAIFSVGGMIGSFVGLFVNRRGR
1lvi_A	LSACIASFIFGYQVSVLNTIKNFIVVEFEWCKGEKDRLSFLLASVFIGAVLGGCGFSGYL.VQFGR
Pho84	RIYGMELIIMIVCTILQTTVAHSPAINFVAVLTFYRIVMGIGIGGDYPLSSIITSEFATTKWRGAI
1pw4_A	VFLPAGLILAAAVMLFMGEVFPWAT..SSIAVMFVLLFLCGWFQGMGWPPCGRTMVHWSQKERGGI
1pv6a	KYLLWIIITGMLVMFAPFFIFIFGPLLQYLVGSIVGGIYLGFCFNAGAPAVEAFIEKVSRRSNE..
1ja5_A	NSMLMMNLLAFVSAVLMGFS...KLGKSFEMILGRFIIGVYCGLTTFGVPMYVGEVSPTAFRGAL
1lvi_A	LSLLIIYNFFFLVSILTSITHFH.....TILFARLLSGFGIGLTVSVPMYISEMTHKDKKAY
Pho84	MGAVFANQAWGQISGGIIALILVAAKYGELEYANSAGAECDARCQKACDQMWIRILIGLGTVLGLACI
1pw4_A	VSVWNCAHNVGGGIPPLLFLGLMAWFN.....DWHAAALYMPAFCAILVA
1pv6a	FGRARMFGCVGWALGASIVGIMFT.....INNQFVFWLGGSCALILA
1ja5_A	GTLHQLGIVVGILIA.....QVFGLD SIMGNKDL.WPILLSIIFIPALLQC
1lvi_A	GVMHQLFITFGIFVAVMLGLA.....MGEKPKADSTEPLTSFAKLWWRLMFLFPSVISLIGILA
Pho84	YFRLTIIPESPRYQLDVNAKLELAAAQEQDGEKKIHDTSDDEMAINGLERASTAVESLDNHPKAS
1pw4_A	LFAFAMMRDTPQSCGLPPIEEYKNDYPDDYNEKAEQELTAKQIFMQYV.....
1pv6a	VLFFAKTDAPSSATVANA.....VGANHSAFS
1ja5_A	IVLPFCPEPRFLINRNEENRAKSVLKKLRGTADVT.....HDLQEMKEESRQMMRE.KKVT
1lvi_A	LNVFFKEETPYFLFEKGRIEESKNILKKIYETDNVDEPLNA.....IKEAVEQNESAKKNS
Pho84	FKDFCRHFGQWKYKILLGTAGSWFTLDVAFYGLSLNSAVILQTIIGYAGSKNVYKKLYDTAVGNLI
1pw4_A	.....PNKLLWYIAIANVFVYLLRYGILDWSPTYLEVKHFDK.....SSWAYF
1pv6a	LKLALFLRQPK....LWFLSLYVIGVSCITYDVFDDQFANFFTSFFATGEQGT.....RVFGYVTT
1ja5_A	ILELFR..SPAYRQPIIAVVLQLSQQLSGINAVFYYSTSIFEKAGVQQ.....PVYATI
1lvi_A	LSLLSALKIPSRYVILGCLLSGLQQFTGINVLVSNSNELYKEFLDSHLI.....TILSV
Pho84	LICAGSLPGYWVSFTVDIIGRKPIQLAGFIILTALFCVIGFAYHKLGDHGLLALYVICQFFQNF
1pw4_A	LYEYAGIPGTLGCGWMSDKVFRGNRGATGVFFMTLVTIATIVYMNPNAGNPTVDMICMIVIGFLIYG
1pv6a	MGELLNASIMFFAPLIINRIIGKNALLLAGTMSVRIIGSSF....ATSALEVVLKTLHMFEVFP
1ja5_A	GSGIVNTAFTVVSFLVVERAGRRRLHLIGLAGMAILMTIALALLEPWMSYLSIVAIFFGVAFVEVG
1lvi_A	VMTAVNFLMTFPAIYIVEKIGRKTLGLLWGCVGVLVAYLPTAIANSNFVKILSIVATFVMIISFAVS
Pho84	PNTTTFIVPGECFPTRYRSTAAGISAASGKVGAIIAQTALGTLDHNCARDGKPTNCWLPVHMEIF
1pw4_A	PVMLIGLHALELAPKKAAGTAAGFTGLFGYLGGSVAASAIVGYTVDFG.....WDGGFMVMI
1pv6a	LLVGCFKYITSQFEVRFSAIYLVCFCCFKLAMIFMSVLAGNMYESIGFQGAYLVGLVALGFTLI
1ja5_A	PGPIPWFIIVAEELFSQGRPAIAVAGFSNWTNFIIV.....GMCFQYVEQLCGPYVFIIF
1lvi_A	YGPVLWIYLHEMFSEIKDASAASLASLVNWCVAIIVVFPDIIKKSPS.....ILFIVFS
Pho84	ALFMLLGIFTTLIPETKRKTLLEEINELYHDEIDPATLNFRNKNNDIESSSPSQLQHEA
1pw4_A	GGSI LAVILLIVMIGEKRRHEQLLQEL.....
1pv6a	SVFTLSGPGPLSLR....ROVNEVA.....
1ja5_A	TVLLVLFIFTYFKVPETKGRTFDEIASGFRQGG.ASQSDKTPEELFHPLGADSQV....
1lvi_A	VMSILTFFFIFFFIKETKGGEIGTSPYITMEERQKHM TKS VV.....

Fig. 1. Alignment of Pho84 with MFS transporters. Pho84 was predicted similar to several MFS transporter structures by a number of well-established secondary structure and fold recognition methods at the MetaServer [18]. The alignment of the sequences is from the joint evaluation of the outcome by the 3D-Jury system. The predicted TM helices of Pho84 are visualized in dark gray, and the established helices of the PDB structures are in light gray (note the lack of fit for some loop regions). The proteins most similar to Pho84 were (in rank) the bacterial glycerol-3-phosphate/phosphate antiporter (GlpT; PDB code 1pw4) and lactose permease (LacY; PDB code 1pv6), the human glucose transporter (GLUT1; PDB code 1ja5a) and the *Plasmodium* hexose transporter (PfhT1; PDB code 1lvi). Boxes depict the conserved MFS signature motifs discussed in Section 3.

domains of the Pho84 could therefore not be modeled onto the GlpT structural template. Consequently, in Fig. 2(a) the structural model is represented by amino acids S52 to K546 of

Pho84. However, it should be noted that TM segment predictions based on hydrophobicity and charge distribution do not always yield the correct number of segments, i.e., the superior



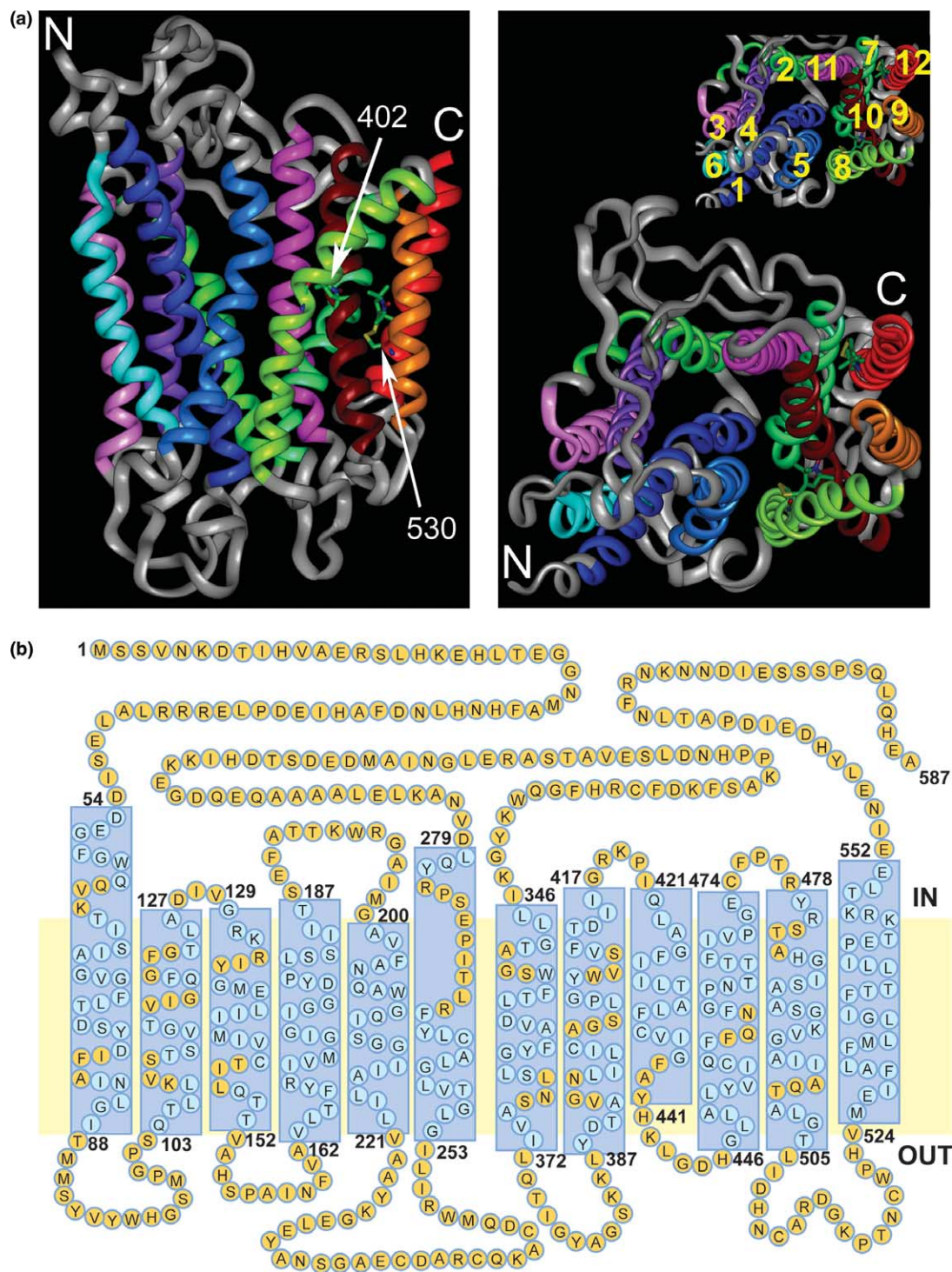


Fig. 2. Structural model of Pho84. (a) Front-view (left) of the Pho84 structure (amino acids S52 to K546) in the plane of the lipid bilayer is shown and also a top-view presentation (right) where the numbering of the individual helices is shown (inset). N and C refer to the N- and C-termini, respectively, of the Pho84. (b) A 2D presentation of the Pho84 based on the 3D structure model. Transmembrane segments are indicated as blue boxes. The secondary structure within the TM domains as predicted by MODELLER using the GlpT template is also highlighted. Most of the residues within the TM domains are on an  $\alpha$  helical backbone (blue circles), whereas series of amino acids predicted to have random coil character are highlighted by yellow circles.

TMHMM method (at [www.cbs.dtu.dk/](http://www.cbs.dtu.dk/)) yielded only nine segments for Pho84 (data not shown).

Several conserved motifs are found in MFS proteins (boxes in Fig. 1). The pentameric amino acid sequence RxGRR (x is any amino acid and R may be replaced by K) is one such motif

commonly found in the loops connecting TM 2 and 3 and also TM 8 and 9 (discussed in [8]). In the human Glut1 glucose transporter, such positive charges found at the corresponding loops have been shown to be important for correct insertion and topological orientation of the immediate TM segments

[22]. The corresponding loops of the GlpT structure contain partly conserved sequences (RsnpR and RnGRf, respectively; [13]) and they are also present in the Pho84 protein (ivGRK between TM 2 and 3 and iiGRK between TM 8 and 9, respectively; Fig. 2(b); [1]), possibly indicating a similar function as an important determinant of the Pho84 protein topology.

Another highly conserved motif that can be found in both halves of the Pho84 protein (PESPR and PETKR in the N- and C-terminal half, respectively) is the PEST-rich sequence. This sequence has been ascribed a role in degradation both in MFS [23] and in ATP-binding cassette [24] proteins. Previously, we have observed that the Pho84 protein undergoes regulated cleavage approximately in the middle of the primary structure of Pho84 [25]. The N-terminal PEST-rich sequence of Pho84 (i.e., PESPR) is localized to positions 271–275. This is at the end of TM 6 in the structure and these amino acids protrude from the membrane domain on the cytosolic side and thus are accessible for modifications by cellular factors.

### 3.2. Production of purified Pho84

Initially, we wished to make use of a previously described bacterial expression system [26] to obtain sufficient amounts of highly purified and solubilized Pho84 for EPR spectroscopic analysis. This setup is based on a single chromatographic purification step where the catalytically active Pho84 protein, fused with an N-terminal consecutive hexa-histidine sequence and an Xpress antibody epitope, is retained on a  $\text{Ni}^{2+}$  column and eluted with an increased concentration of imidazole. In that study, the catalytically active fusion protein was incorporated in liposomes, which, in fact, constituted a second purification step of the transporter. For the present study, however, purified Pho84 protein in a soluble state was preferred. In order to efficiently eliminate contaminating proteins in the 50–300 mM imidazole elution, and thus increase the purity and yield of purified Pho84, a dual affinity expression and purification was elaborated. For this, the *PHO84* gene was inserted in the pTrcHisB expression plasmid together with a flanking sequence encoding the FLAG antibody epitope (DYKDDDDK) at the C-terminal end of Pho84 (Fig. 3). After IPTG induced expression in TOP10F' *E. coli* cells and solubilization of proteins, the total cell protein extract was applied onto the  $\text{Ni}^{2+}$  charged HiTrap column in the presence of imidazole at a concentration of 30 mM (in Tris or sodium-phosphate buffer). After washing with buffer containing 50 mM imidazole, the Pho84 fusion protein was eluted with 300 mM imidazole. The eluted fraction (about 4 ml) contained essentially all Pho84 protein that had initially been retained on the column. In order to remove the remaining contamination proteins, the eluted volume was immediately allowed to pass the anti-FLAG antibody resin twice followed by extensive washing. Finally, competitive binding of pure FLAG peptide to the resin specifically eluted the Pho84 fusion protein (Fig. 3). The eluted volume (4ml) typically containing 1–2 mg of protein (from the 1.7 liter culture) was immediately used for further analysis. The purity and yield were independent on whether Tris or phosphate (not shown) was used as buffering system. A single FLAG affinity purification step (not shown) yielded protein at a lower purity; hence, both chromatographic steps were judged to be necessary. The functional consequence of the FLAG epitope addition to the C-terminal end of Pho84 has been examined in vivo. In that analysis, a pRS416 based plas-

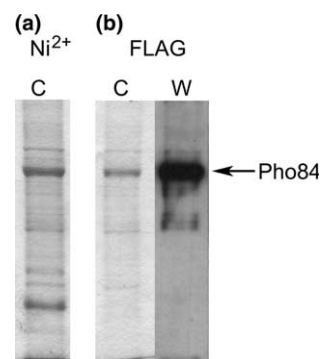


Fig. 3. Dual-affinity purification of Pho84. Protein eluted from the  $\text{Ni}^{2+}$  (a) and FLAG (b) affinity columns were solubilized and separated by SDS-PAGE. The protein purity was analyzed and compared by Coomassie staining (C) and the identity of the Pho84 fusion protein (arrow) was determined by Western blot (W) analysis using both anti-FLAG (shown here) and anti-Xpress (not shown) monoclonal antibodies.

mid construct harboring the *PHO84-FLAG* under control of its natural promoter showed that the Pho84-FLAG has a retained capability to transport phosphate in  $\Delta\text{pho84}$  yeast cells under phosphate limiting conditions (Lagerstedt, Pattison-Granberg and Persson; unpublished results). Similarly, the functionality of the Pho84 protein with the hexa-histidine and Xpress epitope sequences fused to the N-terminus has been demonstrated in a reconstituted system [26].

Several advantages of this dual-affinity system can be identified: (i) using the affinity of the hexa-histidine for chelated  $\text{Ni}^{2+}$  ions as a first, bulk purification method allows for the collection of essentially all extracted Pho84 protein, partly purified and in a reduced volume, (ii) as judged by Western blot analysis, the FLAG antibodies have very low cross-reactivity with endogenous *E. coli* proteins, (iii) the use of two specific affinities effectively diminishes the presence of contaminants in the final protein preparation, (iv) elution with peptide can be performed at physiological pH, and (v) the use of affinity tags at the extreme N- and C-terminal ends ensures that only protein with an intact primary structure is purified.

### 3.3. EPR spectroscopic analysis

Site-directed spin label (SDSL) EPR spectroscopy analysis has proven to be a very powerful technology to study structural aspects of all kinds of proteins [27,28] and other biological molecules such as lipids [29,30], DNA [31] and RNA [32] and also in protein–protein [33] and protein–lipid [34] interaction studies. In particular, SDSL-EPR has been widely used for the elucidation of structural aspects of membrane-spanning proteins, which due to their hydrophobic properties are difficult to analyze with conventional crystallographic technologies, (reviewed in [35]). In these studies, the biological molecule is modified at a chosen location with a sulfhydryl-specific nitroxide reagent to introduce a paramagnetic side-chain. Cysteine residues are commonly utilized for this thiol binding of the nitroxide, an approach that most often is preceded by site-directed mutagenesis.

The primary structure of the Pho84 protein harbors 12 native cysteines. These are located both in the hydrophobic TM regions and in the more hydrophilic loops (Fig. 2(b)). A cysteine free *PHO84* construct where all native cysteines were replaced with serines was previously constructed and shown to



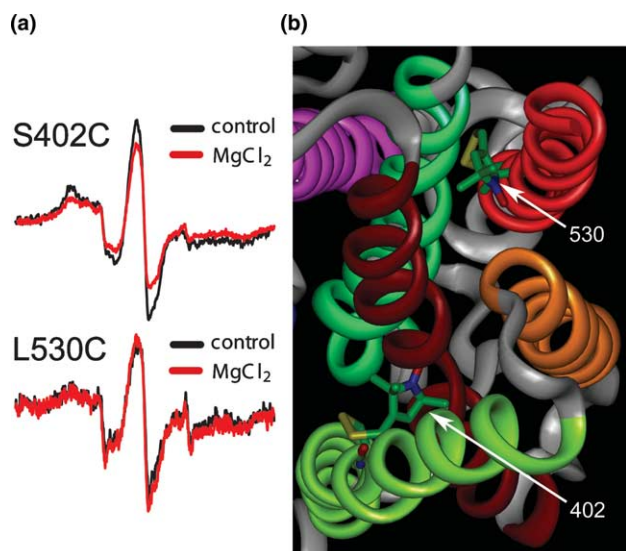


Fig. 4. EPR analysis (a) of S402C and L530C in the presence (red) or absence (black) of 2 mM  $\text{Mg}^{2+}$  together with locations (b) in Silicon Graphics produced structures of local domains.

have an *in vivo* expression and catalytic activity essentially identical to the unmodified Pho84 [14]. Based on this cysteine free *PHO84* template, single cysteine mutants were created in TM segment 8 (TM8; S402C) and TM segment 12 (TM8; L530C). These two locations were chosen to exemplify two TM regions assumingly being part of the inner core (TM8) and outer fence (TM12) of the Pho84 structure.

The detergent-solubilized mutants were MTS spin labeled in the purification process as described in Section 2 and EPR analysis was performed. As can be seen in Fig. 4, the spectra derived from both positions reflect a tightly packed environment. The shapes of these spectra, acquired from spin labeled Pho84 in phosphate buffer, were also obtained from labeled Pho84 in Tris buffer (not shown). Since  $\text{Mg}^{2+}$  is known to affect the functional properties of Pho84 by a drastic reduction of the phosphate uptake capacity [36], we also examined whether the spin labels located on TM 8 or 12 are conformationally sensitive to  $\text{Mg}^{2+}$ . Thus, also shown in Fig. 4 are the EPR spectra of spin labeled S402C and L530C in the presence of 2 mM  $\text{MgCl}_2$ . Since the  $\pm \text{Mg}^{2+}$  samples contain identical amounts of protein, the spectrum of the S402C protein is clearly more broadened in the presence of  $\text{Mg}^{2+}$ , while no significant change is reported from the label located on TM 12. Since similar, albeit less pronounced, response is seen for spin labeled S402C in Tris buffer (not shown), the  $\text{Mg}^{2+}$  effect appears to be phosphate independent. The broadening at position 402 could arise from a further restriction of motion, such as a loss in backbone or side chain dynamics [37]. However, the lack of increased amplitude in the hyperfine extrema or change in the central linewidth suggests an increase in a magnetic dipolar interaction between labels in close proximity, which may be responsible for the  $\text{Mg}^{2+}$ -induced broadening. Thus,  $\text{Mg}^{2+}$  may influence the oligomeric state of Pho84 or the relative arrangement of associated proteins in a complex. Positions within TM8 may therefore be useful for probing conformational dynamics associated with function. In the structurally related protein LacY (cf. above), the corre-

sponding TM 8 seems to be part of a region that is labile to structural changes, i.e., the “rotation” between the first and second halves (two domains) of the protein during membrane insertion in a lipid-modified mutant [38].

Our structural model places both positions 402 and 530 in a tightly packed interior environment. Such buried positions in proteins display a characteristic EPR spectrum with broad splittings when labeled with the MTS spin label employed in these studies [27]. Since the nitroxides at both 402 and 530 report such an environment, we have demonstrated how the model can be directly tested for accuracy. Further probing sites predicted to fall on lipid-exposed faces of the TM domains or in the loop regions with spin labels will confirm whether the sites reflect a more flexible location as predicted.

The combination of our dual-affinity purification system with SDLS EPR spectroscopy, possibly in combination with NMR as described elsewhere [39], will allow us to improve the present model by adding on experimentally determined restraints such as defined distances between residues in the Pho84 structure.

**Acknowledgments:** The Human Frontier Science Organization, the Swedish Research Council, the foundations Lars Hiertas Minne, and Karl and Annie Leons Minnesfond supported this work. J.O.L. received travel fellowships from the Swedish Foundation for International Cooperation in Research and Higher Education, the Foundation Blanceflor Boncompagni-Ludovisi, née Bildt, the foundation Bengt Lundqvist Minne and AstraZeneca.

## References

- [1] Persson, B.L., Lagerstedt, J.O., Pratt, J.R., Pattison-Granberg, J., Lundh, K., Shokrollahzadeh, S. and Lundh, F. (2003) *Curr. Genet.* 43, 225–244.
- [2] Carroll, A.S. and O’Shea, E.K. (2002) *Trends Biochem. Sci.* 27, 87–93.
- [3] Bun-ya, M., Nishimura, M., Harashima, S. and Oshima, Y. (1991) *Mol. Cell. Biol.* 11, 3229–3238.
- [4] Petersson, J., Pattison, J., Kruckeberg, A.L., Berden, J.A. and Persson, B.L. (1999) *FEBS Lett.* 462, 37–42.
- [5] Martinez, P., Zvyagilskaya, R., Allard, P. and Persson, B.L. (1998) *J. Bacteriol.* 180, 2253–2256.
- [6] Saier, M.H. (2000) *Mol. Microbiol.* 35, 699–710.
- [7] Henderson, P.J.F. (1993) *Curr. Opin. Cell Biol.* 5, 708–721.
- [8] Pao, S.S., Paulsen, I.T. and Saier Jr., M.H. (1998) *Microbiol. Mol. Biol. Rev.* 62, 1–34.
- [9] Maiden, M.C., Davis, E.O., Baldwin, S.A., Moore, D.C. and Henderson, P.J. (1987) *Nature* 325, 641–643.
- [10] Rubin, R.A., Levy, S.B., Henrikson, R.L. and Kezdy, F.J. (1990) *Gene* 87, 7–13.
- [11] Griffith, J.K., Baker, M.E., Rouch, D.A., Page, M.G., Skurray, R.A., Paulsen, I.T., Chater, K.P., Baldwin, S.A. and Henderson, P.J. (1992) *Curr. Opin. Cell Biol.* 4, 684–695.
- [12] Abramson, J., Smirnova, I., Kasho, V., Verner, G., Kaback, H.R. and Iwata, S. (2003) *Science* 301, 610–615.
- [13] Huang, Y., Lemieux, M.J., Song, J., Auer, M. and Wang, D.N. (2003) *Science* 301, 616–620.
- [14] Berhe, A., Zvyagilskaya, R., Lagerstedt, J.O., Pratt, J.R. and Persson, B.L. (2001) *Biochem. Biophys. Res. Commun.* 287, 837–842.
- [15] Froncisz, W. and Hyde, J.S. (1982) *J. Magn. Reson.* 47, 515–521.
- [16] Hubbell, W.L., Froncisz, W. and Hyde, J.S. (1987) *Rev. Sci. Instrum.* 58, 1879–1886.
- [17] Laemmli, U.K., Beguin, F. and Gujer-Kellenberger, G. (1970) *J. Mol. Biol.* 47, 69–85.
- [18] Ginalska, K., Elofsson, A., Fischer, D. and Rychlewski, L. (2003) *Bioinformatics* 19, 1015–1018.
- [19] Sali, A. and Blundell, T.L. (1993) *J. Mol. Biol.* 234, 779–815.
- [20] Abramson, J., Kaback, H.R. and Iwata, S. (2004) *Curr. Opin. Struct. Biol.* 14, 413–419.

- [21] Edman, M., Berg, S., Storm, P., Wikström, M., Vikström, S., Öhman, A. and Wieslander, Å. (2003) *J. Biol. Chem.* 278, 8420–8428.
- [22] Sato, M. and Mueckler, M. (1999) *J. Biol. Chem.* 274, 24721–24725.
- [23] Marchal, C., Haguenauer-Tsapis, R. and Urban-Grimal, D. (2000) *J. Biol. Chem.* 275, 23608–23614.
- [24] Martinez, L.O., Agerholm-Larsen, B., Wang, N., Chen, W. and Tall, A.R. (2003) *J. Biol. Chem.* 278, 37368–37374.
- [25] Lagerstedt, J.O., Zvyagilskaya, R., Pratt, J.R., Pattison-Granberg, J., Kruckeberg, A.L., Berden, J.A. and Persson, B.L. (2002) *FEBS Lett.* 526, 31–37.
- [26] Fristedt, U., Weinander, R., Martinsson, H.S. and Persson, B.L. (1999) *FEBS Lett.* 458, 1–5.
- [27] Hubbell, W.L., Gross, A., Langen, R. and Lietzow, M.A. (1998) *Curr. Opin. Struct. Biol.* 8, 649–656.
- [28] Hubbell, W.L., Cafiso, D.S. and Altenbach, C. (2000) *Nat. Struct. Biol.* 7, 735–739.
- [29] Marsh, D. and Horvath, L.I. (1998) *Biochim. Biophys. Acta* 1376, 267–296.
- [30] Subczynski, W.K. and Kusumi, A. (2003) *Biochim. Biophys. Acta* 1610, 231–243.
- [31] Biswas, R., Kuhne, H., Brudvig, G.W. and Gopalan, V. (2001) *Sci. Prog.* 84, 45–67.
- [32] Qin, P.Z. and Dieckmann, T. (2004) *Curr. Opin. Struct. Biol.* 14, 350–359.
- [33] Persson, M., Hammarström, P., Lindgren, M., Jonsson, B.-H., Svensson, M. and Carlsson, U. (1999) *Biochemistry* 38, 432–441.
- [34] Hubert, A., Henderson, P.J.F. and Marsh, D. (2003) *Biochim. Biophys. Acta* 1611, 243–248.
- [35] Kaback, H.R., Sahin-Toth, M. and Weinglass, A.B. (2001) *Nat. Rev. Mol. Cell. Biol.* 2, 610–620.
- [36] Fristedt, U., van der Rest, M., Poolman, B., Konings, W.N. and Persson, B.L. (1999) *Biochemistry* 38, 16010–16015.
- [37] Columbus, L. and Hubbell, W.L. (2002) *Trends Biochem. Sci.* 27, 288–295.
- [38] Bogdanov, M., Heacock, P.N. and Dowhan, W. (2002) *EMBO J.* 21, 2107–2116.
- [39] Spooner, J.R., Veenhoff, L.M., Watts, A. and Poolman, B. (1999) *Biochemistry* 38, 9634–9639.